

Trajectories for Human Missions to Mars, Part 1: Impulsive Transfers

Damon F. Landau* and James M. Longuski†
Purdue University, West Lafayette, Indiana 47907-2023

DOI: 10.2514/1.18995

Earth–Mars trajectories with low energy requirements that also limit the (transfer) time a crew spends in interplanetary space are essential to the design of cost-effective, minimal-risk missions. We compute optimal ΔV trajectories with constraints on the transfer time of flight for launch years 2009 through 2022. We further explore the consequences of specifying different time of flight limits (from 120 to 270 days) for human missions to Mars. In addition to conjunction class trajectories, we calculate free-return, Mars–Earth semicycler, Earth–Mars semicycler, and cycler trajectories. The trades between powered and aeroassisted planetary capture for each trajectory type are also examined. We find that as the number of flybys increase (i.e., free returns have one flyby, semicyclers may have from two to four flybys, and cyclers have an unlimited number of flybys), the V_∞ increase, but the mission mass decreases because less maneuvers are performed by the crew transfer vehicle. The energy requirements of the trajectories decrease with increasing flight times, and the optimal ΔV is reduced by up to 50% when the flight time limit is increased from the NASA-recommended 180 days, to 270 days. Our results are compiled into sets of plots that describe the optimal, constrained time of flight trajectories for use in Mars mission studies.

I. Introduction

THERE have been many investigations into the best way to conduct human missions to Mars [1–20]. Typical mission scenarios are either short duration (about 600 days with 30-day Mars stay time) or long stay time (about 550 days with 900-day mission duration). Opposition class trajectories [21–30] provide transfers for short duration missions, whereas conjunction class trajectories [26–37] are applicable to long stay time missions. (Mars is near opposition at the midpoint of a short duration mission, and Mars passes through conjunction in the middle of a long stay time mission.) In addition to these direct transfers, a mission to Mars could incorporate free-return trajectories [38–45], Mars–Earth semicyclers [46,47], Earth–Mars semicyclers [48], or cyclers [49–54].

Two key issues with human spaceflight are the deleterious effects of zero gravity and radiation. Consequently, the time of flight (TOF) between Earth and Mars is often constrained to reduce the time the crew must spend in interplanetary space. To examine the effects of limiting TOF, we compute optimal ΔV trajectories (to reduce mission cost) with constrained TOF (to reduce mission risk). We consider a range of TOF from 120 to 270 days. Unfortunately, trajectories between Earth and Mars with short TOF, short mission duration, and low-energy requirements (low ΔV) do not exist; thus, we do not include opposition class trajectories in our analysis. Instead, assuming impulsive ΔV , we examine conjunction, free-return, semicycler, and cycler trajectories. The effects of powered versus aeroassisted planetary arrivals are also examined [55–58]. It is assumed that one mission (to Mars and back) occurs once every synodic period. Because Earth–Mars trajectories approximately repeat every seven synodic periods (every 14.95 years), we consider short TOF trajectories over a seven synodic-period cycle (for 2009–2022 Earth departure years).

II. Trajectory Types

A. Conjunction Class

Conjunction class trajectories provide Earth–Mars transfers for three mission scenarios: 1) direct [16], 2) semidirect [17], and 3) stopover [37]. In a direct mission everything (crew, transfer vehicle, etc.) is launched from the Earth’s surface directly toward Mars, where the crew and transfer vehicle land via aeroassisted direct entry. After the 500-day Mars stay time everything is launched off the surface of Mars and the crew returns to Earth using direct entry (when the transfer vehicle is either landed or expended). The semidirect scenario also begins with all mission components on Earth’s surface, but at Mars arrival the transfer vehicle is placed into a parking orbit (either with a powered maneuver or aerocapture) instead of landing on the surface. At Mars departure, the crew rendezvous with the transfer vehicle in orbit then returns to Earth. For stopover missions, the crew begins on Earth, but the transfer vehicle begins in Earth orbit (e.g., from a previous mission). After an in-orbit rendezvous the crew and transfer vehicle leave for Mars, where the crew lands and the transfer vehicle is placed in orbit. Following another in-orbit rendezvous, the crew and transfer vehicle depart for Earth, where the crew lands and the transfer vehicle is placed in Earth orbit for reuse. (A summary of the mission scenarios and trajectories is provided in Table 1.)

A sample mission using conjunction transfers is illustrated in Fig. 1. This particular scenario begins on 26 September 2022 followed by a 180-day transit to Mars. [All subsequent trajectory plots (Figs. 1–5) include an outbound transfer in 2022.] The Mars stay time is 550 days, and the mission concludes on 24 March 2025 after a 180-day inbound transfer.

B. Free Return

Should any incident on the way to Mars preclude the crew from landing (e.g., a propulsion system failure or an injury to a crew member), a free-return trajectory would allow the crew to return to Earth without any major maneuvering (i.e., zero deterministic ΔV). These trajectories are constructed such that if there is no capture maneuver at arrival, a gravity assist from Mars will send the crew and vehicle back to Earth. We examine free-return trajectories for direct, semidirect, and stopover mission scenarios, though free returns may be used (and are often incorporated) in semicycler and cycler scenarios. There are three traditional types of Mars free-return trajectories: 1) opposition/Venus flyby [45], 2) 2:1 Earth:spacecraft resonance [43], and 3) 3:2 Earth:spacecraft resonance [43]. For

Presented as Paper 5095 at the AIAA/AAS Astrodynamics Specialist Conference, Providence, RI, 16–19 August 2004; received 26 July 2005; revision received 21 December 2005; accepted for publication 21 December 2005. Copyright © 2006 by Damon F. Landau and James M. Longuski. Published by the American Institute of Aeronautics and Astronautics, Inc., with permission. Copies of this paper may be made for personal or internal use, on condition that the copier pay the \$10.00 per-copy fee to the Copyright Clearance Center, Inc., 222 Rosewood Drive, Danvers, MA 01923; include the code \$10.00 in correspondence with the CCC.

*Doctoral Candidate, School of Aeronautics and Astronautics, 315 North Grant Street; landau@ecn.purdue.edu. Student Member AIAA.

†Professor, School of Aeronautics and Astronautics, 315 North Grant Street; longuski@ecn.purdue.edu. Associate Fellow AIAA.

Table 1 Summary of Earth–Mars mission scenarios

Architecture	Earth encounter	Mars encounter	Schemata
Direct	Surface	Surface	
Semidirect	Surface	Parking orbit	
Stopover	Parking orbit	Parking orbit	
M–E semicycler	Flyby	Parking orbit	
E–M semicycler	Parking orbit	Flyby	
Cycler	Flyby	Flyby	

constrained TOF and long duration missions (on the order of 3 years) the 3:2 resonance (which has a heliocentric orbit period of 1.5 years) free return provides the lowest average ΔV of the three choices, thus we choose to examine this type in more detail. (We note that the Venus flyby free returns occasionally offer better performance than the 3:2 resonance trajectories, but involve large variations in ΔV over several synodic periods.)

An example 3:2 resonance free-return trajectory is presented in Fig. 2. Because this trajectory was constructed while constraining the Earth–Mars TOF, it no longer adheres to the 3:2 resonance, but still allows a return to Earth with no postlaunch ΔV . Although the free-return abort is available, the nominal mission uses only the Earth–Mars portion of the trajectory. The crew would stay on Mars for about 550 days then take a short TOF inbound trajectory home (e.g., the Mars–Earth transit in Fig. 1).

C. Mars–Earth Semicycler

A transfer vehicle on a Mars–Earth semicycler trajectory begins at Mars (ideally in a loose parking orbit), swings by Earth after orbiting the sun (sans crew), then picks up the next Mars-bound crew and stays in orbit about Mars until the next transfer opportunity. Thus the trajectory sequence is Mars–Earth–Earth–Mars (MEEM). The first trajectory maneuver ejects the transfer vehicle from Mars orbit; no maneuver occurs at Earth arrival (the crew employs aeroentry); a “taxi” vehicle launch transports the crew from Earth to the transfer vehicle (hyperbolic rendezvous); and either a propulsive maneuver or aerocapture achieves Mars orbit insertion. Deep space maneuvers (DSMs) are also often required to maintain the trajectory. We note that one trajectory (the sequence MEEM) is used for both the outbound and inbound transfers to reduce the number of required maneuvers

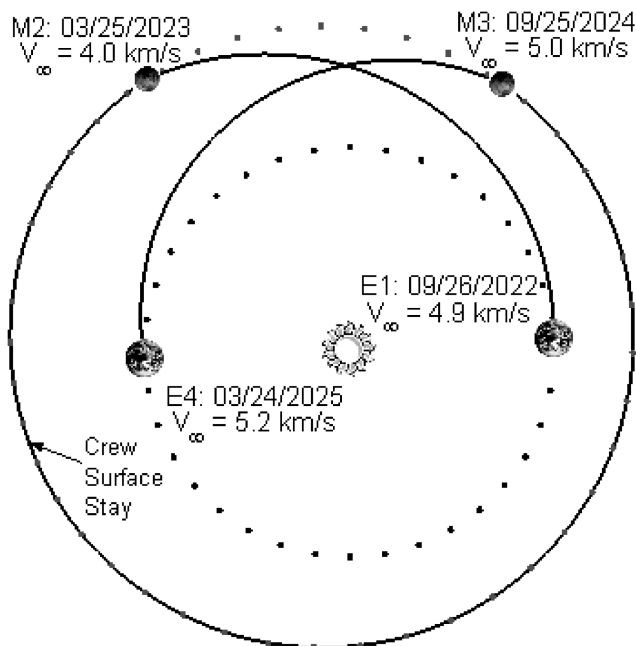


Fig. 1 Outbound and inbound conjunction class transfers.

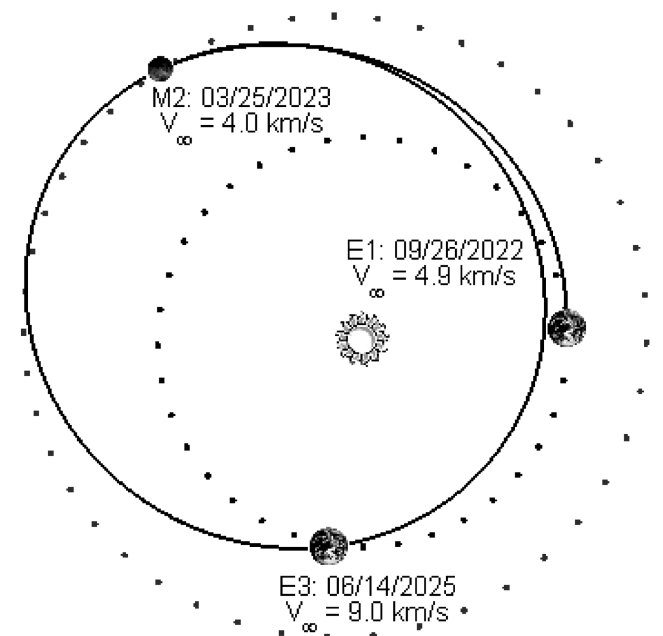
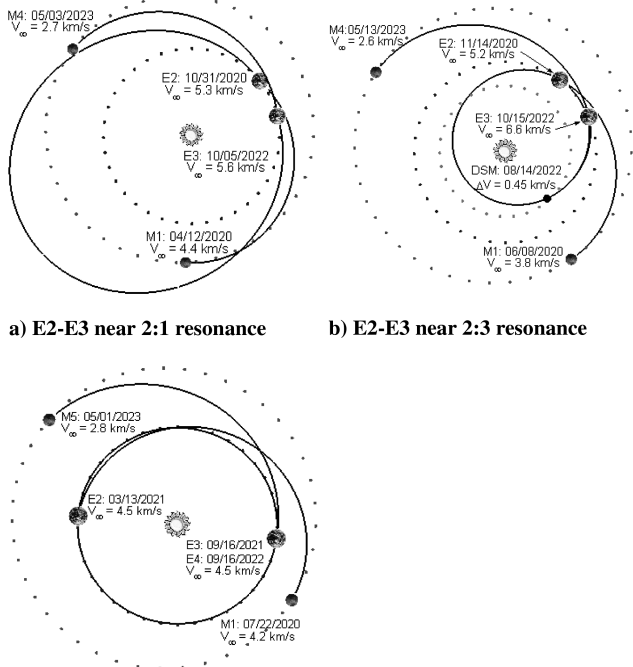


Fig. 2 Mars free-return trajectory with near 3:2 Earth:spacecraft resonance from E1–E3.



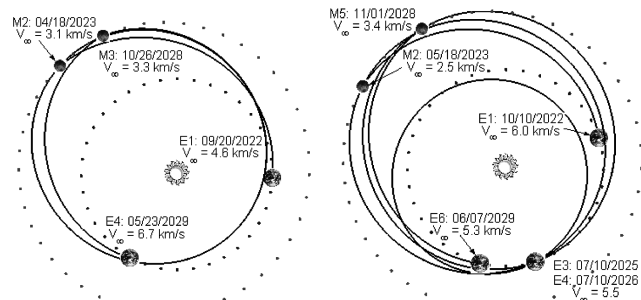
a) E2-E3 near 2:1 resonance b) E2-E3 near 2:3 resonance

c) E2-E4 1.5 year transfer

Fig. 3 Mars–Earth semicyclers.

(and hence the number of ΔV). For example, only one Mars departure maneuver is necessary when the trajectory incorporates both transfers (i.e., Earth–Mars and Mars–Earth), whereas two maneuvers are required when the outbound and inbound trajectories are separate.

The total trajectory duration (from Mars launch to Mars arrival) dictates the number of transfer vehicles required to provide one mission per synodic period. For example, if the total interval is between two and three synodic periods then three vehicles would be required to provide short TOF outbound and inbound transfers each synodic period. We examined two-vehicle [46] and three-vehicle [47] trajectories and found the average ΔV to be comparable, and so we choose the two-vehicle option to reduce cost. There are three types of two-vehicle trajectories that can be distinguished by the Earth–Earth transfer: 1) near 2:1 resonance, 2) near 2:3 resonance, and 3) 1.5-year inclined transfer (with an extra Earth flyby). These three trajectory types are depicted in Fig. 3. The first leg (Mars–Earth) of the trajectory provides the return trip for a mission launched in the previous synodic period. (In the case of Fig. 3 the trajectories begin in 2020, supplying the return for a mission launched from Earth in 2018.) After the Earth–Earth transfer, a new mission begins with a crew transfer to Mars on the final leg of the trajectory (for the 2022 outbound opportunity). We find that the near 2:1 resonance



a) M2-M3 near 3:4 resonance b) E1-E3 near 3:2 resonance,
E3-E4 1:1 resonance, E4-E6
near 3:2 resonance

Fig. 4 Earth–Mars semicyclers.

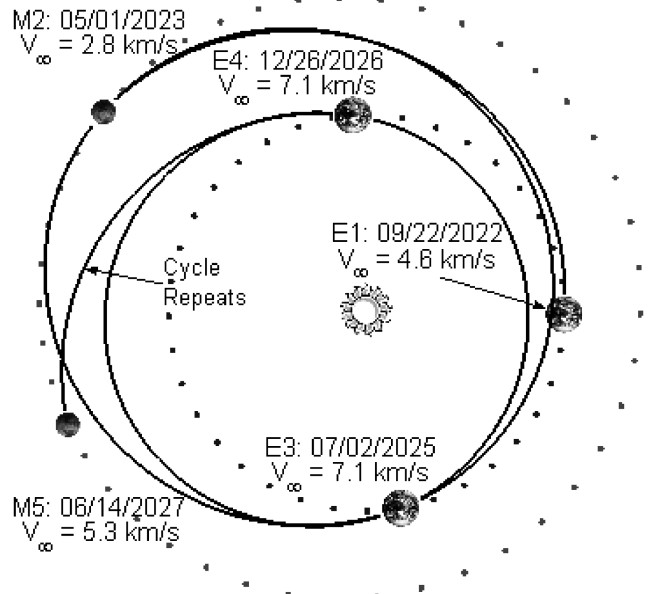


Fig. 5 Outbound cyler trajectory with E1–E3 near 3:2 resonance and E3–E4 near 1.5 year transfer.

type provides the lowest ΔV Mars–Earth semicycler when Mars is near perihelion (during the 2018–2022 Earth–Mars opportunities); the near 2:3 resonance type is most effective when Mars is near aphelion; and the 1.5-year type is best for the longer TOF transfers (when TOF > 230 days). Though the 2:3 resonance type has a perihelion well within Venus’s orbit (see Fig. 3b), the crew will not be on the transfer vehicle at this point, and so they are not exposed to the radiation associated with this portion of the trajectory.

D. Earth–Mars Semicycler

This trajectory is the opposite of the Mars–Earth semicycler; instead of MEEM, the sequence is EMME. The maneuver sequence is thus: transfer vehicle Earth-orbit departure, crew aeroentry at Mars, crew taxi launch and hyperbolic rendezvous with the transfer vehicle at Mars, then propulsive or aerocapture Earth arrival. Additional transfer vehicle DSMs are usually necessary. We identify two classes of Earth–Mars semicyclers: 1) three-vehicle (in which the trajectory duration is between two and three synodic periods) and 2) four-vehicle (in which the total duration is between three and four synodic periods) [48]. One version of a three-vehicle trajectory is based on the trajectory of Chen et al. [53], which has a short TOF Earth–Mars transfer followed by a 2:3 resonance orbit with Mars and ends with a short TOF transfer back to Earth. The other three-vehicle trajectory begins with a 2:1 resonance free-return trajectory (with short Earth–Mars TOF), followed by an Earth gravity assist that places the spacecraft into a half-year inclined transfer and ends with a 2:1 resonance free return (with short Mars–Earth TOF). (This flyby sequence is EMEEME.) We also examined two versions of four-vehicle Earth–Mars semicyclers. The first version employs a short Earth–Mars leg, then a near 3:4 Mars resonance orbit, followed by a short Mars–Earth transfer (as in Fig. 4a). The second version begins with a 3:2 resonance free-return trajectory (with short Earth–Mars TOF), followed by a 1:1 resonance with Earth and ends with a 3:2 resonance free return that provides a short TOF transfer from Mars to Earth (as in Fig. 4b). Thus, these semicyclers are either constructed from a resonant Mars orbit bounded by short TOF legs, or from two free returns (one outbound, one inbound) connected by an Earth–Earth transfer.

We propose these four-vehicle trajectories for Earth–Mars semicycler missions because the ΔV requirements (which correlate to mass and cost) are significantly lower than the three-vehicle ΔV . (Thus four relatively small propulsion systems are chosen over three large ones.) The free-return semicycler is most effective for short

Table 2 Required taxi and transfer vehicle maneuvers for each trajectory type

Trajectory	Earth departure ΔV	Mars arrival ΔV	Mars departure ΔV	Earth arrival ΔV	DSM
Conjunction	Taxi & TV	TV ^a or neither ^b	Taxi & TV	TV ^a or neither ^b	Neither
Free return	Taxi & TV	TV or neither ^b	N/A	N/A	Neither
M–E semicycler ^c	Taxi	TV ^a or neither ^b	Taxi & TV	Neither	TV
E–M semicycler ^c	Taxi & TV	Neither	Taxi	TV ^a or neither ^b	TV
Cyclers ^c	Taxi	Neither	Taxi	Neither	TV

^aPowered capture. ^bAeroassisted capture. ^cThe one-time transfer vehicle launch ΔV is ignored.

transfers (when TOF < 150 days) and when Mars is near aphelion (during the 2009 and 2022 outbound opportunities), whereas the near 3:4 resonance semicycler is best for longer TOF transfers. Figure 4 presents an example of both four-vehicle trajectory versions.

E. Cyclers

Cycler trajectories regularly encounter Earth and Mars, but do not stop at either planet (i.e., they continue in orbit about the sun indefinitely). The essential maneuvers in a cycler mission are crew taxi launches at Mars and Earth to rendezvous with the transfer vehicle plus any DSMs required to maintain the cycler orbit. Because the crew lands via direct entry and the transfer vehicle never enters a parking orbit, there is no ΔV cost for planetary arrivals. We examined two-vehicle [51], three-vehicle [53], and four-vehicle cyclers [52,54] and we found the latter to require the least ΔV , which makes four-vehicle cyclers attractive for use in Mars missions. (Again, the initial investment of launching extra vehicles subsequently results in lower mass missions.) An example outbound cycler trajectory is given in Fig. 5, where we note that the cycle is a repetition of the sequence Earth–Mars–Earth (so we have EME EME . . .). There is also a corresponding inbound cycler, which provides short TOF Mars–Earth transfers.

III. Trajectory Models

We model the heliocentric trajectories as point-to-point conics with instantaneous V_∞ rotations at planetary encounters. The minimum allowable flyby altitude at Earth and Mars is 300 km. Deep space maneuvers are also modeled as instantaneous changes in the heliocentric velocity. We do not allow maneuvers within the sphere of influence of a flyby planet because of the operational difficulty in achieving an accurate ΔV during a gravity assist. We assume that planetary departure and arrival maneuvers occur at 300 km above the planet’s surface, thus the ΔV for escape or capture is

$$\Delta V = \sqrt{V_\infty^2 + 2\mu/r_p} - \sqrt{2\mu/r_p} \quad (1)$$

where μ is the gravitational parameter of the planet and r_p is the periapsis radius of the escape or capture hyperbola (in this case 300 km above the surface radius). Although Eq. (1) explicitly provides the ΔV to achieve a V_∞ magnitude from a parabola, this ΔV is sufficient to optimize interplanetary transfers that begin on the surface or in a parking orbit. The difference between the true ΔV and the value from Eq. (1) is found by subtracting the launch trajectory or parking orbit velocity at r_p from the periapsis velocity of the parabola. Because this difference is independent of the interplanetary transfer (both the parking orbit and the parabola are planetocentric trajectories), it does not affect the outcome of the optimal trajectory. (In other words, the difference is merely a constant bias.)

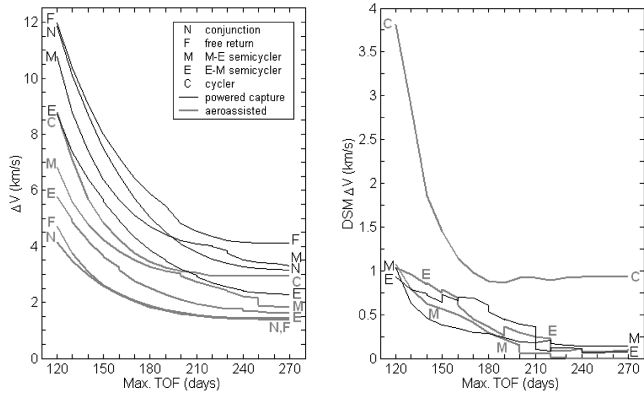
The sequence of maneuvers included in the optimal ΔV calculation is summarized in Table 2 for each trajectory type. If the crew taxi, transfer vehicle (TV), or both vehicles perform a maneuver (when the maneuvers are required is provided in Table 2), the weighting on the corresponding ΔV is unity, and if no maneuver is performed then the weighting is zero. Throughout this paper we assume the semicycler or cycler transfer vehicle is already in a parking orbit or on an interplanetary trajectory; thus, we ignore the initial transfer vehicle launch cost for these trajectories. Most semicycler and cycler assessments do not include taxi ΔV in the cost

function, which often results in ballistic trajectories (with no DSMs). Balancing the taxi ΔV against the TV ΔV (as in Table 2), however, usually leads to nonzero DSMs and lower V_∞ . Although these relative weightings (one or zero) do not explicitly minimize mission mass or cost, the resulting trajectories are representative of those that result from more detailed analyses (e.g., one that includes the relative vehicle masses). A key benefit of our weighting system is that we only rely on natural parameters (planetary orbits and masses) for computations, yet we retain trajectory features (i.e., low V_∞ and low ΔV) that are essential for effective integrated mission design.

We use a sequential quadratic programming algorithm [59] to compute minimum- ΔV trajectories with bounded TOF. (The departure and arrival dates may vary, but the TOF between them is less than or equal to the bound.) Similar methods have been used in the optimization of the Galileo trajectory to and at Jupiter and the Cassini trajectory to Saturn [60,61]. We optimize Earth–Mars trajectories so that the total ΔV over the entire 15-year cycle is minimized (as opposed to, say, minimizing the maximum ΔV during the cycle). Though the arrival V_∞ for aerocapture is often limited (e.g., below 9 km/s at Earth [56] and below 7 km/s at Mars [57]), we did not constrain the V_∞ ; in this way we analyze the lowest possible ΔV trajectories. We decide if and when to incorporate additional DSMs for impulsive transfers via Lawden’s primer vector analysis [62,63]. For each trajectory type, we initially optimized the long TOF (270-day) trajectory for the 2009 outbound opportunity. The 270-day TOF trajectory served as the initial guess for the 260-day TOF trajectory, and so on (by 10-day intervals) until the 120-day TOF transfer was optimized. The whole process was then repeated for the subsequent synodic periods up to the 2022 outbound opportunity. In the case of cyclers, multiple synodic periods were optimized together because the trajectory is continuous. We employed a similar process from 120 to 270-day TOF (and vice versa) to optimize the semicycler and cycler trajectories.

IV. Results

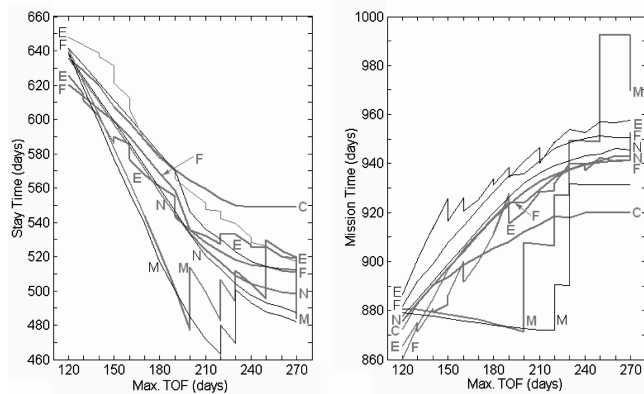
The optimal ΔV for a given TOF fluctuates significantly over the seven-synodic-period cycle (about 15 years) due to the eccentricity and inclination of Mars’s orbit. Usually, the largest- ΔV missions occur when Mars is near aphelion (during the 2009 opportunity), and the smallest- ΔV missions occur when Mars is near perihelion (during the 2016 opportunity). For a given TOF, the maximum- ΔV mission corresponds to the smallest Mars payload mass, while the minimum- ΔV mission provides an opportunity to send the most payload to Mars. Alternatively, the maximum- ΔV mission is correlated to the longest TOF necessary to land a given payload at Mars, while the minimum- ΔV opportunity sets the lower bound on TOF over the synodic cycle. Because the mission requirements vary significantly over the 15-year cycle, it is necessary to calculate trajectory data for each of the seven launch opportunities (2009–2022) to derive average and maximum values. The average values provide an estimate of the mission cost over several synodic periods, whereas the maximum trajectory values set an upper bound for the design of mission components. For example, the maximum Earth departure V_∞ would size the launch vehicle upper stage, and the maximum Mars arrival V_∞ would size the heat shield or propulsive-capture system at Mars. We note that the maximum trajectory requirements do not occur during the same launch opportunity; thus they are better suited to the design of mission components rather than an analysis of comprehensive mission scenarios.



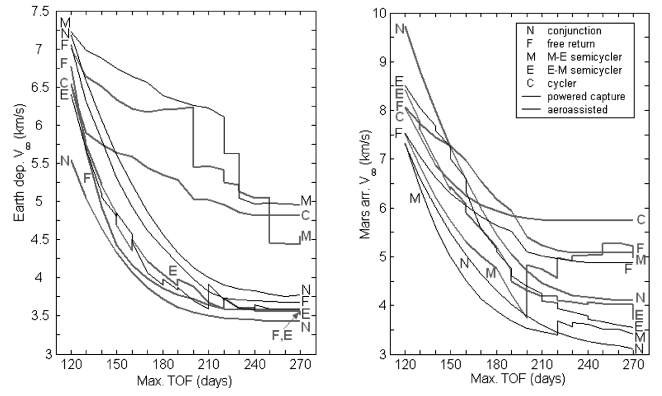
a) Total optimized ΔV b) DSM ΔV
Fig. 6 Average ΔV over 15-year cycle.

The key mission parameters include the optimal total ΔV , the arrival and departure V_∞ at Earth and at Mars, the DSM ΔV , the Mars stay time, and the total mission duration. These eight parameters are plotted as functions of the maximum allowable TOF in Figs. 6–8 (which provide average performance) and in Figs. 9–11 (which provide maximum values). These average and maximum values are derived from the Earth–Mars trajectories that span the seven launch opportunities between 2009 and 2022 (where details are provided in [64]). We compute the root-mean square of the V_∞ in Fig. 8 because it leads to a better estimate of the average mission ΔV than the V_∞ mean. There is an ambiguity in how to charge the DSM ΔV in semicycler and cycler trajectories because these trajectories span multiple synodic periods (e.g., an Earth–Mars semicycler starting in 2009 flies by Mars twice and returns to Earth in 2016, spanning three synodic periods). To resolve this ambiguity, we allocate the Earth–Mars semicycler DSM ΔV to the mission on which the Earth–Mars leg begins, and the Mars–Earth semicycler DSM ΔV is charged to the mission on which the Mars–Earth leg concludes. (Thus any DSMs that occur between 2009 and 2016 for an Earth–Mars semicycler are charged to the 2009 mission.) In the case of cyclers, we resolve the ambiguity as follows: any cycler DSMs that occur between the Earth encounters that precede or follow a crew transfer leg (Earth–Mars or Mars–Earth) are allocated to that mission.

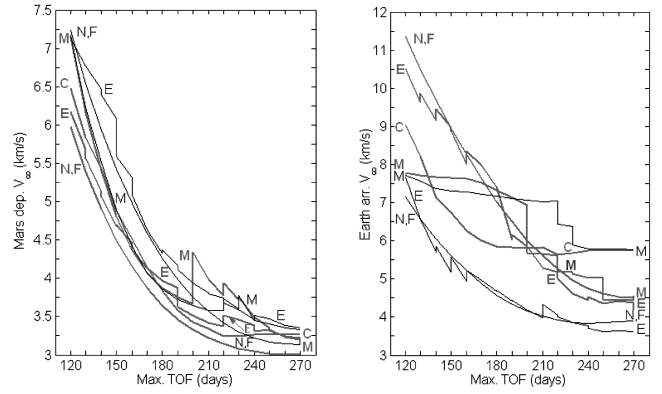
The thin black lines and the thick gray lines in Figs. 6–11 denote the powered or aeroassisted capture option in Table 2, respectively. In our formulation, powered arrivals are not necessary for cycler missions; thus, there is no distinction between aeroassisted and powered cycler trajectories. A sharp jump (a vertical line) in the data indicates a change in trajectory type. For example, the jump in ΔV from 3 to 4 km/s at 190 days TOF for the aeroassisted Earth–Mars semicyclers in Fig. 9a is a result of the optimal outbound trajectory switching from the near 4:3 resonance version (Fig. 4a) to the free-return version (Fig. 4b) in 2009 (as also shown in [64], Fig. 15a).



a) Mars stay time b) Total mission duration
Fig. 7 Average stay time and mission time over 15-year cycle.



a) Earth departure b) Mars arrival

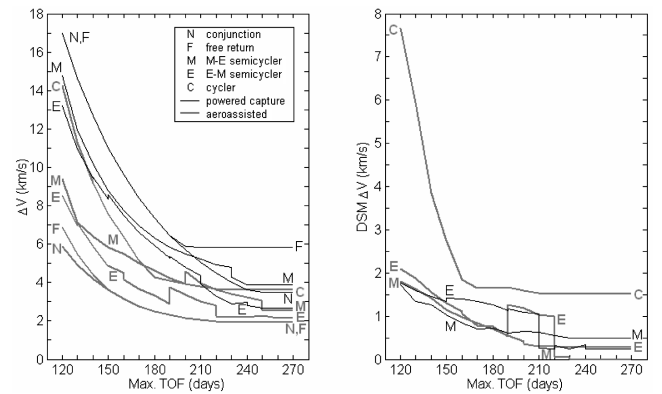


c) Mars departure d) Earth arrival
Fig. 8 Root-mean square V_∞ over 15-year cycle.

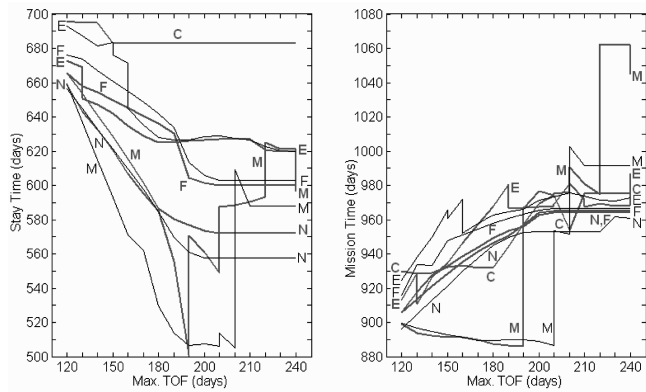
A horizontal line indicates that the optimal trajectory is no longer constrained by the TOF bound (e.g., TOF = 220 through 270 days for powered free returns in Fig. 9a) and the optimal TOF is below the constrained limit.

Although the total ΔV is the key factor for optimization, the other trajectory parameters provide additional insight for analyzing Mars mission scenarios.

As an example, we examine the average cycler mission with the TOF constrained below 210 days. For cycler missions the escape energy required by the crew taxi to rendezvous with the cycling transfer vehicle depends on the departure V_∞ [5.0 km/s at Earth (Fig. 8a) and 3.3 km/s at Mars (Fig. 8c)]. The arrival V_∞ [5.8 km/s at Mars (Fig. 8b) and 5.8 km/s at Earth (Fig. 8d)] size the heat shield that decelerates the taxi to a safe surface landing. The DSM ΔV [0.78 km/s (Fig. 6b)] indicates the propulsion system requirements of the transfer vehicle. Finally, the Mars stay time [560 days (Fig. 7a)] provides a time allotment for surface exploration, and the



a) Total optimized ΔV b) DSM ΔV
Fig. 9 Maximum ΔV over 15-year cycle.



a) Mars stay time b) Total mission duration
Fig. 10 Maximum stay time and mission time over 15-year cycle.

mission duration [915 days (Fig. 7b)] determines the time that the crew spends away from Earth and the amount of consumables needed to sustain them. Similarly, other mission scenarios may be examined by applying the corresponding trajectory data in Figs. 6–11.

The variation in total ΔV (e.g., Fig. 6a) among the trajectory types is mainly attributed to the different number of maneuvers in the cost function (summarized in Table 2). For example, powered-capture conjunction trajectories have four maneuvers in the ΔV calculation (Earth departure, Mars arrival, Mars departure, and Earth arrival), whereas aeroassisted capture conjunction trajectories include only two maneuvers (Earth departure and Mars departure). In fact, all of the aeroassisted capture trajectories share the same cost function (Earth and Mars departure plus DSM ΔV). Usually, the ΔV -rank order (from lowest to highest) is conjunction, free-return, Earth–Mars semicycler, Mars–Earth semicycler, and finally cyclus.

The powered-capture conjunction and free-return trajectories also share identical cost functions and their ΔV are nearly identical except during the 2014 (for TOF above 180 days), 2016, and 2018 (for TOF

below 200 days) launch opportunities [64]. The key reason for the difference in ΔV (between conjunction and free-return trajectories) is that the Mars-flyby V_∞ must be relatively high to complete the free return to Earth (with no DSMs). In fact, during the 2016 launch opportunity the V_∞ is never below 7.5 km/s. To account for the higher Mars V_∞ , the Earth departure V_∞ are usually lower for free returns than for conjunction trajectories. On the other hand, aeroassisted trajectories do not include the arrival V_∞ in the ΔV -cost function, and the conjunction and free-return average ΔV is within a few percent, especially when the TOF is greater than 150 days. As a result, incorporating the free-return abort option in a human mission to Mars with direct aeroentry does not change the ΔV requirements significantly, yet reduces the risk to the crew. The main disadvantage of these free-return trajectories is that, in the event of abort, the crew does not return to Earth until after 1080 days, that is, 3 years (on average) instead of the 930-day nominal mission duration.

In comparison to the other trajectory types, optimal Mars–Earth semicyclers tend to have higher Earth V_∞ and lower Mars V_∞ , whereas the V_∞ of Earth–Mars semicyclers are closer to the conjunction counterparts (within 10% on average). The cyclus Earth departure V_∞ are usually much larger (around 40% greater) than the conjunction case, but the Mars departure V_∞ are often much lower (only 5% above the conjunction V_∞), primarily because of DSMs that precede the Mars flyby. Because the cyclus-arrival V_∞ do not vary as a function of TOF as much as the conjunction trajectories do, the arrival V_∞ for cyclers are significantly lower (by about 20%) for short TOF and are much higher (by about 30%) for long TOF when compared to the conjunction V_∞ . Often, the Earth–Mars semicycler DSM ΔV are larger than the Mars–Earth semicycler DSM ΔV for short TOF, and are slightly lower for long-TOF trajectories. The cyclus DSM ΔV are significantly larger than (i.e., at least double) the DSM ΔV of semicyclers. We note that there are ballistic (i.e., DSM $\Delta V = 0$) versions of the semicycler and cyclus trajectories, but the inclusion of V_∞ in the cost function results in nonzero DSMs to minimize the total ΔV . The Mars stay time and total mission duration do not vary significantly among the trajectory types (for a given transfer TOF) with the exception of Mars–Earth semicyclers, which have notably lower stay times and mission durations for low to moderate TOF and have mission durations in excess of 1000 days for TOF above 240 days during the 2016 and 2020 launch opportunities. Also, cyclers tend to have slightly longer stay times (an average of 50 days longer) than the other optimized trajectories.

The fundamental advantage of aeroassisted capture is that a heat shield is often considerably less massive than the propellant required to decelerate a vehicle at planetary arrival. As a result, less mass must be launched from Earth, which ultimately reduces mission cost. A secondary benefit of direct entry or aerocapture is that the departure V_∞ is reduced significantly below the powered-capture case (at the expense of higher arrival V_∞). For example, conjunction and free-return departure V_∞ for aeroassisted trajectories range from about 20% (for short TOF) to 10% (for long TOF) below the powered-capture V_∞ at either Earth or Mars. However, this benefit becomes less pronounced for short TOF trajectories if arrival- V_∞ limits are required (to satisfy entry guidance and heating constraints), but the combination of negligible propellant cost at arrival and reduced departure energy still provides a distinct advantage over powered-capture missions. The V_∞ reduction is not as prominent for semicycler trajectories, which always have at least one aeroassisted arrival. (Mars–Earth semicyclers employ direct entry at Earth and Earth–Mars semicyclers employ direct entry at Mars.) As a result, the Mars departure V_∞ for Mars–Earth semicyclers and the Earth departure V_∞ for Earth–Mars semicyclers do not change significantly between aeroassisted and powered-capture trajectories. There is a notable difference on the other short TOF transfer, where the Earth departure V_∞ for Mars–Earth semicyclers is reduced by 10% (on average) and the Mars departure V_∞ for Earth–Mars semicyclers decreases by 10–20% when comparing the aeroassisted to the powered-capture trajectories.

As expected, the optimal ΔV and V_∞ decrease as the TOF upper limit is increased, and the stay time decreases and the mission duration increases as the TOF becomes larger. We note that the

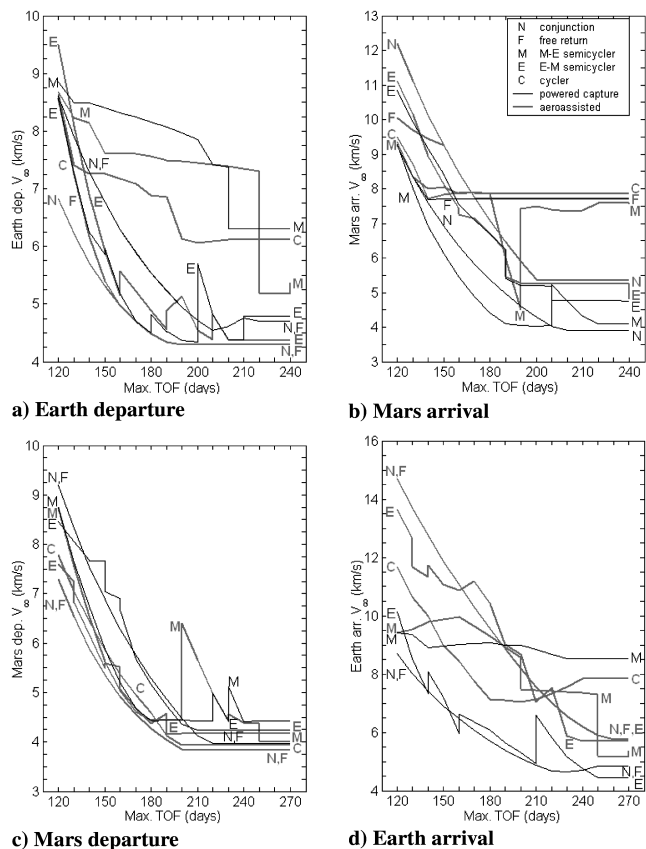


Fig. 11 Maximum V_∞ over 15-year cycle.

ΔV increases dramatically for short TOF trajectories. For example, the ΔV for most trajectories doubles from 270-day TOF to 150-day TOF, then triples (with respect to 270-day TOF) at TOF of only 130 days. Notable exceptions include conjunction and Earth–Mars semicycler powered-capture trajectories, which double around 180-day TOF and triple at 150-day TOF for the maximum- ΔV transfers. Consequently, the same amount of ΔV is saved by extending the TOF by 20 days from 130- to 150-day TOF as is saved by allowing the TOF to increase by 120 days from 150- to 270-day TOF, on average.

Further, when the maximum TOF is extended from 180 days up to 270 days, the relative ΔV savings range from 15–45% for average missions, and up to 65% of the ΔV is eliminated for the maximum- ΔV missions (which are usually during the 2009 or 2022 launch opportunities). Alternatively, the absolute reduction in ΔV (from 180- to 270-day TOF) is around 1.5 km/s for powered capture and 0.75 km/s for aeroassisted capture, with up to 4 km/s reduction in the maximum ΔV . Also, the average ΔV reduction is 10–20% when the TOF is extended by only 30 days from 180 to 210 days, which translates to an absolute ΔV savings of around 1 km/s for powered-capture and 0.4 km/s for aeroassisted trajectories with up to a 2 km/s reduction in the maximum ΔV . We note that the ΔV savings is usually much less during opportunities when Mars is near perihelion (namely, 2016–2018).

The maximum departure V_∞ for aeroassisted conjunction trajectories (Fig. 11a for Earth and Fig. 11c for Mars) establish a lower bound on the V_∞ required to reach Mars from Earth (or vice versa) for every launch opportunity. For example, the maximum Earth departure V_∞ for 180-day TOF is 4.5 km/s. If an upper stage for Mars missions only provides an excess velocity of 4.3 km/s for a given payload, then the nominal mission is not always available; either the payload must be reduced or the TOF must be extended (at the expense of some additional shielding or structure mass for artificial gravity) during the more demanding launch years (in this case 2009 and 2022). Similar lower bounds may be determined for any desired TOF between 120 and 270 days using the aeroassisted conjunction-trajectory curves in Fig. 11.

Though semicycler and cycler trajectories typically require higher V_∞ and higher ΔV than conjunction trajectories, the mass requirements (e.g., initial mass in low-Earth orbit or total propellant mass) for semicycler and cycler missions are usually lower because the relatively massive transfer vehicle (which contains radiation shielding, interplanetary life-support systems, crew accommodations, etc.) performs fewer maneuvers [20]. (Again, we ignore the one-time cost of launching a semicycler or cycler transfer vehicle.) For example, direct, semidirect, and stopover missions (which are summarized in Table 1) are constructed so that the transfer vehicle performs between two to four maneuvers (as given in Table 2), whereas semicycler transfer vehicles perform two to three maneuvers and cycler vehicles perform only one. [The transfer vehicle requirements are even less for ballistic (DSM $\Delta V = 0$) trajectories.] In essence, more of the mission ΔV is executed by the crew taxis in semicycler and cycler missions than with missions that incorporate conjunction trajectories. As a result, less dry mass (from the transfer vehicle) and less propellant mass (from the elimination of maneuvers) is launched from Earth or Mars, and smaller (or fewer) launch vehicles and upper stages are required to complete the mission. The net mass savings depends on several design factors (such as the mass ratio of the crew transfer vehicle to the taxi), but the data compiled in Figs. 6–11 and in [64] provide the basic trajectory characteristics necessary for mission analyses and trade studies.

V. Conclusions

To further explore the available options for human missions to Mars, we have calculated the minimum- ΔV conjunction, free-return, Mars–Earth semicycler, Earth–Mars semicycler, and cycler trajectories with the stipulation that each trajectory must provide a short TOF transfer (from 120 to 270 days) from Earth to Mars and back. All seven launch opportunities during the 2009–2022 synodic-period cycle are included in our analysis. The 2009 and 2022 launch

opportunities (when Mars is near aphelion) require the most ΔV , whereas the 2016 and 2018 launch years (when Mars is near perihelion) often provide the lowest ΔV transfers. Among the five trajectory types, the rank order in terms of V_∞ and ΔV requirements (from lowest to highest) is conjunction, free-return, Earth–Mars semicycler, Mars–Earth semicycler, and cycler. Because the ΔV for free-return trajectories are usually similar to the conjunction trajectory ΔV , this additional safety feature may be incorporated into Mars missions at relatively little cost. In the free-return case, the total mission time is similar to the conjunction-trajectory mission time, but in the event of abort the crew must remain in space for up to 3 years. We also find that aeroassisted trajectories require significantly lower departure V_∞ and higher arrival V_∞ when compared to powered-capture trajectories.

Though the most efficient way to guard a crew from the hazards of radiation and zero gravity during a Mars mission is still unresolved, additional prophylactics such as artificial gravity or radiation shielding could replace propellant mass (through the reduction of ΔV) by extending the TOF beyond six months. For example, at the expense of one month of additional TOF (to 210 days), the ΔV is reduced by 10–20% on average or up to about 2 km/s of ΔV , whereas a three-month extension to 270 days results in an average savings of 15–45% with up to 4 km/s of ΔV eliminated from the mission. Similar trades in TOF may be performed among the various Earth–Mars trajectory options, which have been compiled for the first time with respect to a maximum allowable flight time.

These optimal trajectory characteristics are particularly useful for preliminary design studies of impulsive missions to Mars, but are inadequate to design missions that incorporate low-thrust technology. The slow acceleration and extended burn time with low-thrust propulsion result in trajectories that are distinct from their impulsive counterparts, requiring a different optimization process for low-thrust transfers. We explore some distinguishing characteristics of low-thrust trajectories for the human exploration of Mars in Part 2.

Acknowledgments

The first author's work has been sponsored in part by a National Defense Science and Engineering Graduate (NDSEG) Fellowship and a National Science Foundation Graduate Research Fellowship.

References

- [1] Burgess, E., *Rocket Propulsion: With an Introduction to the Idea of Interplanetary Travel*, Chapman and Hall, London, 1952, pp. 172–179.
- [2] Von Braun, W., *The Mars Project*, University of Illinois Press, Urbana, IL, 1953.
- [3] Stuhlinger, E., "Electrical Propulsion System for Space Ships with Nuclear Power Source," *Journal of the Astronautical Sciences*, Pt. 1, Vol. 2, Winter 1955, pp. 149–152; Pt. 2, Vol. 3, Spring 1956, pp. 11–14; Pt. 3, Vol. 3, Summer 1956, p. 33.
- [4] Ehrlicke, K. A., Whitlock, C. M., Chapman, R. L., and Purdy, C. H., "Calculations on a Manned Nuclear Propelled Space Vehicle," ARS Rept. 532-57, 1957.
- [5] Irving, J. H., and Blum, E. K., "Comparative Performance of Ballistic and Low-Thrust Vehicle for Flight to Mars," *Vistas in Astronautics*, Vol. II, Pergamon Press, Oxford, U.K., 1959, pp. 191–218.
- [6] Himmel, S. C., Dugan, J. F., Luidens, R. W., and Weber, R. J., "A Study of Manned Nuclear-Rocket Missions to Mars," *Aerospace Engineering*, Vol. 20, July 1961, pp. 18, 19, 51–58.
- [7] Gillespie, R. W., Ragsac, R. V., and Ross, S. E., "Prospects for Early Manned Interplanetary Flights," *Astronautics and Aerospace Engineering*, Vol. 1, Aug. 1963, pp. 16–21.
- [8] Dixon, F. P., "The EMPIRE Dual Planet Flyby Mission," *AIAA/NASA Conference on Engineering Problems of Manned Interplanetary Travel*, AIAA, New York, 1963, pp. 3–18.
- [9] King, J. C., Shelton, R. D., Stuhlinger, E., and Woodcock, G. R., "Study of a Nerva-Electric Manned Mars Vehicle," *AIAA/AAS Stepping Stones to Mars Meeting*, AIAA, New York, 1966, pp. 288–301.
- [10] Bell, M. W. J., "An Evolutionary Program for Manned Interplanetary Exploration," *Journal of Spacecraft and Rockets*, Vol. 4, No. 5, 1967, pp. 625–630.
- [11] Hoffman, S. J., Friedlander, A. L., and Nock, K. T., "Transportation Mode Performance Comparison for a Sustained Manned Mars Base," AIAA Paper 86-2016, 1986.

- [12] Cohen, A., *The 90 Day Study on the Human Exploration of the Moon and Mars*, U.S. Government Printing Office, Washington, D.C., 1989.
- [13] Braun, R. D., and Biersch, D. J., "Propulsive Options for a Manned Mars Transportation System," *Journal of Spacecraft and Rockets*, Vol. 28, No. 1, 1991, pp. 85–92.
- [14] Walberg, G., "How Shall We Go to Mars? A Review of Mission Scenarios," *Journal of Spacecraft and Rockets*, Vol. 30, No. 2, 1993, pp. 129–139.
- [15] Niehoff, J. C., and Hoffman, S. J., "Pathways to Mars: An Overview of Flight Profiles and Staging Options for Mars Missions," AAS Paper 95-478, 1995, *Science and Technology Series of the American Astronautical Society*, Vol. 86, Univelt, Inc., San Diego, CA, 1996, pp. 99–125.
- [16] Zubrin, R., and Wagner, R., *The Case for Mars*, Simon and Schuster, Inc., New York, 1996.
- [17] Hoffman, S., and Kaplan, D. (eds.), *Human Exploration of Mars: The Reference Mission of the NASA Mars Exploration Study Team*, SP 6107, NASA, 1997.
- [18] Drake, B. G. (ed.), *Reference Mission Version 3.0 Addendum to the Human Exploration of Mars: The Reference Mission of the NASA Mars Exploration Study Team*, Exploration Office Document EX 13-98-036, June 1998.
- [19] Donahue, B. B., and Cupples, M. L., "Comparative Analysis of Current NASA Human Mars Mission Architectures," *Journal of Spacecraft and Rockets*, Vol. 38, No. 5, 2001, pp. 745–751.
- [20] Landau, D. F., and Longuski, J. M., "Comparative Assessment of Human Missions to Mars," AAS/AIAA *Astrodynamic Specialist Conference*, AAS Paper 03-513, 2003.
- [21] Sohn, R. L., "Venus Swingby Mode for Manned Mars Missions," *Journal of Spacecraft and Rockets*, Vol. 1, No. 5, 1964, pp. 565–567.
- [22] Titus, R. R., "FLEM—Flyby-Landing Excursion Mode," AIAA Paper 66-36, 1966.
- [23] Deerwester, J. M., and Dhaem, S. M., "Systematic Comparison of Venus Swingby Mode with Standard Mode of Mars Round Trips," *Journal of Spacecraft and Rockets*, Vol. 4, July 1967, pp. 904–911.
- [24] Gillespie, R. W., and Ross, S., "Venus-Swingby Mode and Its Role in the Manned Exploration of Mars," *Journal of Spacecraft and Rockets*, Vol. 4, Feb. 1967, pp. 170–175.
- [25] Casalino, L., Colasurdo, G., and Pastrone, D., "Optimization Procedure for Preliminary Design of Opposition-Class Mars Missions," *Journal of Guidance, Control, and Dynamics*, Vol. 21, No. 1, 1998, pp. 134–140.
- [26] Breakwell, J. V., Gillespie, R. W., and Ross, S. E., "Researches in Interplanetary Flight," *ARS Journal*, Vol. 31, No. 2, 1961, pp. 201–207.
- [27] Knip, G., and Zola, C. L., "Three-Dimensional Trajectory Analysis for Round-Trip Mission to Mars," NASA TN-D-1316, 1962.
- [28] Ross, S., *Planetary Flight Handbook*, SP-35, NASA, 1963.
- [29] Lee, V. A., and Wilson, S. W., "A Survey of Ballistic Mars-Mission Profiles," *Journal of Spacecraft and Rockets*, Vol. 4, No. 2, 1967, pp. 129–142.
- [30] Young, A. C., Mulqueen, J. A., and Skinner, J. E., "Mars Exploration, Venus Swingby and Conjunction Class Mission Modes, Time Period 2000–2045," NASA TM-86477, 1984.
- [31] Gravier, J. P., Marchal, C., and Culp, R. D., "Optimal Trajectories Between Earth and Mars in Their True Planetary Orbits," *Journal of Optimization Theory and Applications*, Vol. 9, Feb. 1972, pp. 120–136.
- [32] Hoffman, S. J., McAdams, J. V., and Niehoff, J. C., "Round Trip Trajectories for Human Exploration of Mars," AAS Paper 89-201, 1989.
- [33] Soldner, J. K., "Round Trip Mars Trajectories: New Variations on Classic Mission Profiles," AIAA Paper 90-2932, Aug. 1990.
- [34] George, L. E., and Kos, L. D., "Interplanetary Mission Design Handbook: Earth-to Mars Mission Opportunities and Mars-to-Earth Return Opportunities 2009–2024," NASA TM-1998-208533, 1998.
- [35] Munk, M. M., "Departure Energies, Trip Times, and Entry Speeds for Human Mars Missions," American Astronautical Society, AAS Paper 99-103, 1999.
- [36] Miele, A., and Wang, T., "Optimal Transfers from an Earth Orbit to a Mars Orbit," *Acta Astronautica*, Vol. 45, No. 3, 1999, pp. 119–133.
- [37] Penzo, P., and Nock, K., "Earth-Mars Transportation Using Stop-Over Cyclers," AIAA Paper 2002-4424, 2002.
- [38] Crocco, G. A., "One Year Exploration Trip Earth-Mars-Venus-Earth," *Proceedings of the 10th International Astronautical Federation*, Springer-Verlag, Vienna, Austria, 1956.
- [39] Battin, R. H., "The Determination of Round-Trip Planetary Reconnaissance Trajectories," *Journal of Aerospace Sciences*, Vol. 26, No. 9, 1959, pp. 545–567.
- [40] Ruppe, H. O., *Interplanetary Flight*, Handbook of Astronautical Engineering, edited by H. H. Koelle, McGraw-Hill, New York, 1961, pp. 9.32–9.44.
- [41] Hénon, M., "Interplanetary Orbits which Encounter the Earth Twice," *Bulletin Astronomique*, Vol. 3, No. 3, 1968, pp. 377–393.
- [42] Wolf, A. A., "Free Return Trajectories for Mars Missions," AAS Paper 91-123, 1991.
- [43] Patel, M. R., Longuski, J. M., and Sims, J. A., "Mars Free Return Trajectories," *Journal of Spacecraft and Rockets*, Vol. 35, No. 3, 1998, pp. 350–354.
- [44] Miele, A., Wang, T., and Mancuso, S., "Optimal Free-Return Trajectories for Moon Missions and Mars Missions," *Journal of the Astronautical Sciences*, Vol. 48, Nos. 2–3, 2000, pp. 183–206.
- [45] Okutsu, M., and Longuski, J. M., "Mars Free-Returns via Gravity Assist from Venus," *Journal of Spacecraft and Rockets*, Vol. 39, No. 1, 2002, pp. 31–36.
- [46] Bishop, R. H., Byrnes, D. V., Newman, D. J., Carr, C. E., and Aldrin, B., "Earth-Mars Transportation Opportunities: Promising Options for Interplanetary Transportation," AAS Paper 00-255, 2000.
- [47] Aldrin, B., Byrnes, D., Jones, R., and Davis, H., "Evolutionary Space Transportation Plan for Mars Cycling Concepts," AIAA Paper 2001-4677, 2001.
- [48] Landau, D. F., and Longuski, J. M., "Mars Exploration via Earth-Mars Semi-Cyclers," AAS Paper 05-269, 2005.
- [49] Hollister, W. M., "Castles in Space," *Astronautica Acta*, Vol. 14, No. 2, 1969, pp. 311–316.
- [50] Rall, C. S., and Hollister, W. M., "Free-Fall Periodic Orbits Connecting Earth and Mars," AIAA Paper 71-92, 1971.
- [51] Byrnes, D. V., Longuski, J. M., and Aldrin, B., "Cycler Orbit Between Earth and Mars," *Journal of Spacecraft and Rockets*, Vol. 30, No. 3, May–June 1993, pp. 334–336.
- [52] Byrnes, D. V., McConaghy, T. T., and Longuski, J. M., "Analysis of Various Two Synodic Period Earth-Mars Cycler Trajectories," AIAA Paper 2002-4423, 2002.
- [53] Chen, K. J., McConaghy, T. T., Landau, D. F., and Longuski, J. M., "A Powered Earth-Mars Cycler with Three Synodic-Period Repeat Time," AAS Paper 03-510, 2003 [*Journal of Spacecraft and Rockets* (to be published)].
- [54] McConaghy, T. T., Yam, C. H., Landau, D. F., and Longuski, J. M., "Two-Synodic-Period Earth-Mars Cyclers with Intermediate Earth Encounter," AAS Paper 03-509, 2003 [*Journal of Spacecraft and Rockets* (to be published)].
- [55] Braun, R. D., Powell, R. W., and Hartung, L. C., "Effect of Interplanetary Options on a Manned Mars Aerobrake Configuration," NASA TP-3019, Aug. 1990.
- [56] Striepe, S. A., Braun, R. D., Powell, R. W., and Fowler, W. T., "Influence of Interplanetary Trajectory Selection on Earth Atmospheric Velocity of Mars Missions," *Journal of Spacecraft and Rockets*, Vol. 30, No. 4, 1993, pp. 420–425.
- [57] Striepe, S. A., Braun, R. D., Powell, R. W., and Fowler, W. T., "Influence of Interplanetary Trajectory Selection on Mars Atmospheric Velocity," *Journal of Spacecraft and Rockets*, Vol. 30, No. 4, 1993, pp. 426–430.
- [58] Lyne, J. E., Wercinski, P., Walberg, G., and Jits, R., "Mars Aerocapture Studies for the Design Reference Mission," AAS Paper 98-110, 1998.
- [59] *Optimization Toolbox User's Guide*, The MathWorks, Inc., Natick, MA, 2004.
- [60] D'Amario, L. A., Byrnes, D. V., Sackett, L. L., and Stanford, R. H., "Optimization of Multiple Flyby Trajectories," AAS Paper 79-162, 1979.
- [61] Sauer, C. G., "Optimization of Interplanetary Trajectories with Unpowered Planetary Swingbys," AAS Paper 87-424, 1987.
- [62] Lawden, D. F., *Optimal Trajectories for Space Navigation*, Butterworths, London, 1963.
- [63] Jezewski, D. J., "Primer Vector Theory and Applications," NASA TR-R-454, Nov. 1975.
- [64] Landau, D. F., and Longuski, J. M., "A Reassessment of Trajectory Options for Human Missions to Mars," AIAA Paper 2004-5095, 2004.